Stability and Decentralized Control of Plug-and-Play DC Distribution Grids

van der Blij, Nils H.; Ramirez-Elizondo, Laura M.; Spaan, Matthijs T.J.; Bauer, Pavol

DOI
10.1109/ACCESS.2018.2875758

Publication date
2018

Document Version
Final published version

Published in
IEEE Access

IEEE Access
SPECIAL SECTION ON ADVANCES IN CHANNEL CODING FOR 5G AND BEYOND

Received September 21, 2018, accepted October 1, 2018, date of publication October 12, 2018, date of current version November 19, 2018.

Digital Object Identifier 10.1109/ACCESS.2018.2875758

Stability and Decentralized Control of Plug-and-Play DC Distribution Grids

NILS H. VAN DER BLIJ[1], (Student Member, IEEE), LAURA M. RAMIREZ-ELIZONDO[1], (Member, IEEE), MATTHIJS T. J. SPAAN[2], (Member, IEEE), AND PAVOL BAUER[1], (Senior Member, IEEE)

[1]Department of Electrical Sustainable Energy, Delft University of Technology, 2628 CD Delft, The Netherlands
[2]Department of Software Technology, Delft University of Technology, 2628 CD Delft, The Netherlands

Corresponding author: Nils H. van der Blij (n.h.vanderblij@tudelft.nl)

This work was supported by the framework of the joint programming initiative ERA-Net Smart Grids Plus through the European Union's Horizon 2020 Research and Innovation Programme.

ABSTRACT Changes in distribution grids pose significant challenges with respect to the control and management of these grids. Stability and decentralized control are vital to ensure the availability and accessibility of plug-and-play dc distribution grids that are (temporarily) without communication. Therefore, this paper presents guidelines for these grids that ensure global stability and a decentralized control strategy that implements these stability guidelines. The stability guidelines are derived using a Brayton–Moser representation of the system to arrive at a Lyapunov candidate function. Furthermore, the decentralized control strategy implements these stability guidelines and ensures that the voltages in the system remain within a specified range. In addition, several simulations are performed to illustrate the stability of the system and the behavior of the control strategy under different scenarios.

INDEX TERMS DC distribution grid, decentralized control, microgrid, plug-and-play, stability.

I. INTRODUCTION

Future distribution grids are likely going to be subjected to changes such as the increasing participation of distributed energy resources (DER), segmentation of the grid (into microgrids), and increasing participation of consumers, producers and prosumers. These changes pose significant challenges with respect to the control and management of distribution grids [1]–[3].

Firstly, the location of power generation is fundamentally changing. The renewable power generation plants are located in regions of high resource availability, rather than regions of high consumption. Furthermore, because of decentralized generation, the power flow in the system is no longer unidirectional [4], [5]. Secondly, the inertia of future distribution systems is significantly less than current grids. Solar and wind energy provide little (rotational) inertia to grids compared to conventional generation, which is still dominant in present-day grids [6], [7]. A costly solution would be to add virtual inertia by incorporating a large amount of storage into the grid. An alternative is to adapt the control to ensure the supply and demand are balanced on a much shorter time scale. Lastly, the uncertainty in the distribution grid is increased. With the increasing participation of renewable energy sources, not only demand is subject to uncertainty, but also supply. Moreover, because of the islanding and de-islanding of microgrids, the topology of the distribution network is also becoming more dynamic [5], [8], [9].

Nevertheless, it is paramount that the distribution system's availability, affordability, accessibility and safety are ensured. To do so, the actors (e.g., loads, sources and storage) in the distribution system must cooperate to find a dynamic balance between supply and demand. Moreover, like the situation in current grids, it is desirable that the distribution grid operates in a plug-and-play fashion [10], [11].

It becomes attractive to employ dc distribution systems since they have several advantages to ac distribution systems with respect to control. DC distribution grids do not require the synchronization (of frequency and phase) or reactive power governance, and do not face challenges regarding harmonic and inrush currents. Therefore, the interconnection of dc (micro)grids is significantly simpler [12], [13]. Furthermore, dc distribution grids are also foreseen to have advantages over ac in terms of efficiency, distribution lines, and converters [14]–[16]. However, the field of dc distribution grids is still relatively novel and more research on the control and protection of these grids is vital.

One significant control challenge is the stability and control of plug-and-play dc distribution grids without communication. This is relevant for systems that aim to be more reliable or cost-effective by not utilizing a communication infrastructure, or for systems that are (temporarily) without communication (for example) due to a fault.

Previous studies on the stability of dc distribution grids often do not ensure global stability, or only apply to well-defined systems (i.e., systems with known topology and/or parameters) or systems that utilize some form of communication. For example, (non-)linear droop based strategies are commonly used for many systems [17]–[22]. Although droop-based strategies do not require any communication they do not ensure global stability unless the system parameters and topology are known. Furthermore, several strategies exist that adapt the virtual impedance or operating mode of the converters depending on system parameters [23]–[29]. These methods further improve stability when flexibility is available in the system, but still rely on well-defined system parameters (e.g., load power) or communication for global stability.

Several plug-and-play control strategies have been presented in previous research. For example, local controllers can be updated after a change in the system occurs [30]. Alternatively, a (centralized) power management strategy can specify the set points of the converters in the grid [31]. Moreover, global stability can be ensured when a well-defined topology is used [26], [32], [33]. However, all these control strategies require some form of communication or that the different system topologies and/or parameters are predefined.

The contributions of this paper are easy-to-use global (small-signal) stability guidelines, a decentralized control strategy that implements these stability guidelines, and supplementary converter guidelines for plug-and-play dc distribution grids that are (temporarily) without communication. Based on the work presented in [34] and [35], the global stability guidelines are derived using a Brayton-Moser representation of the system to arrive to a Lyapunov candidate function. The derived guidelines only pose requirements on the output capacitors of constant power loads and the disconnection of these loads at specified (local) voltages. Furthermore, a decentralized control strategy is presented that establishes global stability and ensures that voltage stays within a specified range. Moreover, three guidelines for converter behavior are presented that further improve the transient behavior of the system. Additionally, several simulations are performed to illustrate the stability and the behavior of the decentralized control strategy.

The remainder of this paper is organized as follows: in Section II the models that are used for the dc distribution system are given. In Section III the stability guidelines for plug-and-play dc distribution systems are derived. In Section IV these guidelines are applied in a novel decentralized control strategy and additional desirable converter guidelines are given. In Section V several simulations are performed to illustrate the global stability of the system and the behavior of the decentralized control strategy. In Section VI the results, and main merits of the work are discussed. Lastly, in Section VII conclusions are drawn.

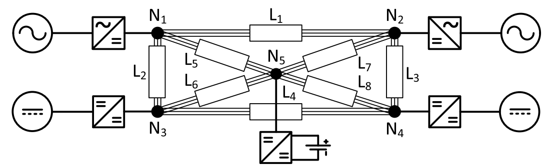

FIGURE 1. Example of a (subsection of a) bipolar dc distribution system containing storage, sources and loads.

II. DC DISTRIBUTION SYSTEM MODEL

An example of a (subsection of a) bipolar dc distribution system is shown in Figure 1. Any dc distribution systems can be described by its n nodes, l distribution lines and o phase conductors. For the sake of simplicity, the dc distribution systems in this paper have a single phase conductor (i.e., are monopolar systems). However, the models described in this section can be extended to multiple phase conductors [36].

A. DC DISTRIBUTION NETWORK MODEL

The incidence matrix, $\boldsymbol{\Gamma}$, is used to describe the electrical network as a directed graph and is given by

$$\boldsymbol{\Gamma}(j,i) = \begin{cases} 1 & \text{if } I_j \text{ is flowing from node } i \\ -1 & \text{if } I_j \text{ is flowing to node } i \end{cases}, \tag{1}$$

where the indices i and j are used to indicate the nodes and lines of the system respectively. Therefore, I_j indicates the current flowing in distribution line j.

For the modelling of the system's lines a lumped element π model is used. This model is valid when the length of the line is much smaller than the wavelength of the signals [36], [37]. The dynamic behavior of dc distribution systems can then be described by the differential equations of their node voltages and line currents, which are given by

$$\boldsymbol{C}\dot{\boldsymbol{U}}_{\boldsymbol{N}} = \boldsymbol{I}_{\boldsymbol{N}} - \boldsymbol{\Gamma}^T \boldsymbol{I}_{\boldsymbol{L}}, \tag{2}$$

$$\boldsymbol{L}\dot{\boldsymbol{I}}_{\boldsymbol{L}} = \boldsymbol{\Gamma}\boldsymbol{U}_{\boldsymbol{N}} - \boldsymbol{R}\boldsymbol{I}_{\boldsymbol{L}}, \tag{3}$$

where $\boldsymbol{U_N}$ are the node voltages, $\boldsymbol{I_L}$ are the line currents, $\boldsymbol{I_N}$ are the sums of the currents from the converters connected to each node, and $\boldsymbol{C}$, $\boldsymbol{L}$ and $\boldsymbol{R}$ are the capacitance, inductance and resistance matrices respectively [36].

B. POWER ELECTRONIC CONVERTER MODELS

In this paper it is assumed that the bandwidths of the power electronic converters are large enough that they react instantaneously to changes in the system [38].

Constant voltage and constant current behavior exhibit no incremental impedance and therefore do not influence (small-signal) stability. Furthermore, constant impedance and constant power loads exhibit positive and negative incremental impedance respectively [39].

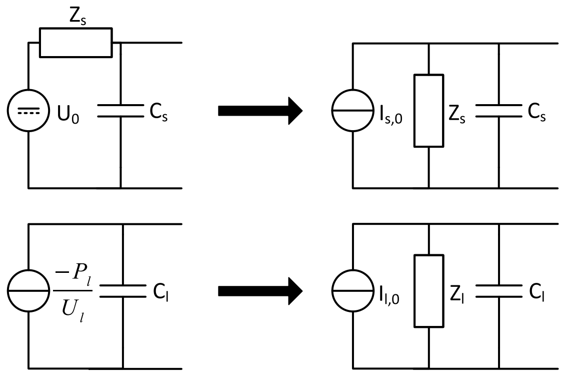

FIGURE 2. **Equivalent circuits of droop controlled sources (top) and constant power loads (bottom).**

Since droop sources can be reduced mathematically to voltage sources and the presence of constant impedance loads is decreasing, droop controlled sources and constant power loads are considered to be the main contributors to the (in)stability of dc distribution grids.

Droop and constant power load converters of the dc distribution systems can be modelled according to the equivalent circuits shown in Figure 2 on the left. The currents flowing from the droop source and constant power load converter into the node are respectively given by

$$I_s = \frac{U_0 - U_i}{Z_s}, \tag{4}$$

$$I_l = -\frac{P_l}{U_n}, \tag{5}$$

where U_0 is the reference voltage, U_i is voltage of the node the converter is connected to, Z_s is the (virtual) impedance of the droop controller, and P_l is the load's power.

For small-signal analysis of the stability, droop sources and constant power loads are modelled as a current source with an impedance in parallel. Furthermore, the constant power load is linearized around a voltage $\overline{U}$. The small-signal behavior of these converters can then be approximated by

$$I_s = \frac{U_0}{Z_s} - \frac{U_i}{Z_s} = I_{s,0} - \frac{U_i}{Z_s}, \tag{6}$$

$$I_l = -\frac{2P_l}{\overline{U}} + \frac{P_l}{\overline{U}^2}U_i = \frac{2\overline{U} - U_i}{Z_l} = I_{l,0} - \frac{U_i}{Z_l}, \tag{7}$$

where Z_l is the equivalent impedance of the constant power load converter and $\overline{U}$ is the voltage at which the load is linearized [35], [40]. The equivalent circuits of these (small-signal) models of droop sources and constant power loads are shown in Figure 2 on the right.

C. DC DISTRIBUTION SYSTEM MODEL

From (2), (3), (6) and (7) the state-space model of the whole dc distribution system is derived to be

$$\dot{X} = \begin{bmatrix} -\boldsymbol{C}^{-1}\boldsymbol{Z}^{-1} & -\boldsymbol{C}^{-1}\boldsymbol{\Gamma}^T \\ \boldsymbol{L}^{-1}\boldsymbol{\Gamma} & -\boldsymbol{L}^{-1}\boldsymbol{R} \end{bmatrix} X + \begin{bmatrix} \boldsymbol{C}^{-1} \\ \emptyset \end{bmatrix} \boldsymbol{I_{N,0}}, \tag{8}$$

where $\boldsymbol{Z}$ is the (diagonal) matrix containing the converter impedances, $\emptyset$ is an empty set, $\boldsymbol{I_{N,0}}$ is the matrix containing the constant terms ($I_{c,0}$) of the converters' (small-signal) model, and

$$\boldsymbol{X} = \begin{bmatrix} \boldsymbol{U_N} \\ \boldsymbol{I_L} \end{bmatrix}. \tag{9}$$

III. DC DISTRIBUTION SYSTEM STABILITY

DC distribution systems are stable if the left-hand matrix in (8) only has eigenvalues with negative real parts. However, the derivation of these eigenvalues is, in general, complex and highly dependent on the incidence matrix $\boldsymbol{\Gamma}$ and accordingly on the topology of the system [40]. Therefore, stability for plug-and-play operation (unknown system topologies) must be derived using an alternative method.

In this section the stability of plug-and-play dc systems is derived. First, the existence and adequacy of an equilibrium is determined using the state-space equations. Second, guidelines for asymptotic stability are derived using a Brayton-Moser representation of the system, which provides a Lyapunov function.

A. EXISTENCE OF AN EQUILIBRIUM

At the equilibrium of the system all time derivatives in the system are zero. Therefore, from (8) the state variables at the equilibrium are given by

$$\boldsymbol{X} = \begin{bmatrix} -\boldsymbol{C}^{-1}\boldsymbol{Z}^{-1} & -\boldsymbol{C}^{-1}\boldsymbol{\Gamma}^T \\ \boldsymbol{L}^{-1}\boldsymbol{\Gamma} & -\boldsymbol{L}^{-1}\boldsymbol{R} \end{bmatrix}^{-1} \begin{bmatrix} -\boldsymbol{C}^{-1} \\ \emptyset \end{bmatrix} \boldsymbol{I_{N,0}}. \tag{10}$$

Using some matrix manipulations the node voltages are found to be

$$\boldsymbol{U_N} = (\boldsymbol{Z}^{-1} + \boldsymbol{\Gamma}^T \boldsymbol{R}^{-1} \boldsymbol{\Gamma})^{-1} \boldsymbol{I_{N,0}}, \tag{11}$$

which is equivalent to finding equivalent impedance of the network topology [35]. Nevertheless, providing sufficient and necessary conditions for the existence of this inverse for any topology (unknown $\boldsymbol{\Gamma}$) is infeasible.

However, sufficient conditions for the existence of an equilibrium are available. According to [34] and [41], an equilibrium is guaranteed to exist if the total load power of the network is bound by

$$P_\Sigma \leq \frac{U_0^2}{4R_\Sigma}, \tag{12}$$

where P_Σ is the total load power of the network, U_0 is the reference voltage of source(s) in the system and R_Σ is the total resistance of the network.

This sufficient condition for the existence of an equilibrium can be substantiated and slightly appended by utilizing a simple example circuit shown in Figure 3. For this equivalent circuit the voltage at the load side's output capacitance is given by

$$U_l = U_0 - \frac{P_l Z_s}{U_l} - \frac{P_l R'}{U_l}, \tag{13}$$

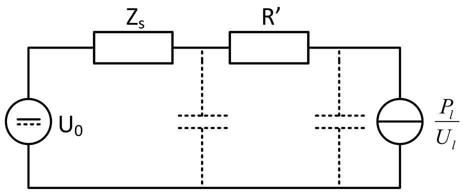

FIGURE 3. Equivalent steady state circuit of a droop controlled source connected to a constant power load via an arbitrary dc distribution network.

where R' is the equivalent resistance of the arbitrary dc distribution network between the source and the load.

A solution for the equilibrium of this system exists if

$$P_l \leq \frac{U_0^2}{4(Z_s + R')}. \tag{14}$$

Now a dc distribution grid with an arbitrary number of constant power loads is considered. In the worst-case scenario the current from all the constant power loads flow through all line resistances. Consequently, the existence of an equilibrium in the worst case scenario can be ensured by

$$P_\Sigma \leq \frac{U_0^2}{4(Z_s + R_\Sigma)}. \tag{15}$$

B. ADEQUACY OF THE EQUILIBRIUM

Equation (15) ensures the existence of an equilibrium, but does not ensure that the voltage in the system remains within predefined limits. Therefore, it must be ensured that the voltage remains above the minimum voltage $U_{\min}$.

In the worst (allowed) case the load current is given by $I_l = \frac{P_l}{U_{\min}}$ and therefore, using the same example circuit from Figure 3, the equilibrium is above the minimum voltage if

$$U_0 - \frac{P_l Z_s}{U_{\min}} - \frac{P_l R'}{U_{\min}} \geq U_{\min}. \tag{16}$$

Equivalently to the existence of the equilibrium, the worst-case scenario is when all load current flows through all the resistance in the network. Therefore the adequacy of the equilibrium in the worst case scenario is ensured by

$$P_\Sigma \leq \frac{U_{\min}(U_0 - U_{\min})}{Z_s + R_\Sigma}, \tag{17}$$

which, as long as the minimum voltage is not chosen to be exactly half of the reference voltage, is more strict than (15).

C. BRAYTON-MOSER REPRESENTATION

To assess the asymptotic stability of dc distribution systems Lyapunov's method is used. From the system's (2) and (3) the natural Lyapunov function candidate is given by

$$\Phi_0 = G_0 - \frac{1}{2}\boldsymbol{I_L}^T \boldsymbol{R} \boldsymbol{I_L} + \boldsymbol{I_L}^T \boldsymbol{\Gamma} \boldsymbol{U_N}, \tag{18}$$

$$G_0 = \sum_i \left(P_{l,i} \ln U_i - \frac{2U_i U_0 - U_i^2}{2Z_{s,i}} + \frac{U_i^2}{2Z_{z,i}} - U_i I_{I,i} \right), \tag{19}$$

where G_0 is the resistive co-content of the sources and loads [34]. The different terms in (19) are for constant power, droop, constant impedance and constant current converters that are connected to each node respectively.

The dynamic equations of the system, (2) and (3), can then be rewritten as

$$\boldsymbol{Q_0}\dot{\boldsymbol{X}} = -\partial_{\boldsymbol{X}} \Phi_0, \tag{20}$$

$$\boldsymbol{Q_0} = \begin{bmatrix} \boldsymbol{C} & \emptyset \\ \emptyset & -\boldsymbol{L} \end{bmatrix}. \tag{21}$$

However, Lyapunov function candidate Φ_0 is not sufficient to ensure stability of the system, since it is not sign definite. Therefore, a closely related Brayton-Moser potential Φ is defined, which is given by

$$\Phi = \frac{\tau_{\max}}{2}(\partial_{\boldsymbol{X}} \Phi_0)^T \begin{bmatrix} \boldsymbol{C} & \emptyset \\ \emptyset & \boldsymbol{L} \end{bmatrix}^{-1} (\partial_{\boldsymbol{X}} \Phi_0) + \Phi_0, \tag{22}$$

where $\tau_{\max}$ is the maximum time constant (L/R) of all the distribution lines in the dc distribution system [34], [42], [43].

Subsequently, by substituting $\dot{\boldsymbol{X}} = -\boldsymbol{Q_0}^{-1} \partial_{\boldsymbol{X}} \Phi_0$ into (22) and utilizing $\boldsymbol{Q}\dot{\boldsymbol{X}} = -\partial_{\boldsymbol{X}} \Phi$, the Brayton-Moser potential Φ and the matrix $\boldsymbol{Q}$ corresponding to to the Brayton-Moser potential Φ are found to be

$$\partial_{\boldsymbol{X}} \Phi = \tau_{\max}(\partial_{\boldsymbol{X}}^2 \Phi_0)^T \begin{bmatrix} \boldsymbol{C} & \emptyset \\ \emptyset & \boldsymbol{L} \end{bmatrix}^{-1} \partial_{\boldsymbol{X}} \Phi_0 + \partial_{\boldsymbol{X}} \Phi_0, \tag{23}$$

$$\boldsymbol{Q} = \begin{bmatrix} \tau_{\max} \partial_{\boldsymbol{X}} \partial_{\boldsymbol{X}} G_0 + \boldsymbol{C} & \tau_{\max} \boldsymbol{\Gamma}^T \\ -\tau_{\max} \boldsymbol{\Gamma} & \tau_{\max} \boldsymbol{R} - \boldsymbol{L} \end{bmatrix}. \tag{24}$$

The Lyapunov function V that follows from this Brayton-Moser representation is given by

$$V = \dot{\boldsymbol{X}}^T \boldsymbol{Q} \dot{\boldsymbol{X}}, \tag{25}$$

which according to LaSalle's invariance principle makes the system asymptotically stable if

$$\dot{V} = \dot{\boldsymbol{X}}^T (\dot{\boldsymbol{Q}} - \partial_{\boldsymbol{X}} \partial_{\boldsymbol{X}} \Phi) \dot{\boldsymbol{X}} \leq 0, \tag{26}$$

$$\boldsymbol{Q} \succ 0. \tag{27}$$

Both of these conditions result in different requirements on the system, which are derived in the following subsections.

D. SYSTEM CONVEXITY

The first condition for asymptotic stability is given by (26). It can be shown that this equation reduces to

$$(\dot{\boldsymbol{Q}} - \partial_{\boldsymbol{X}} \partial_{\boldsymbol{X}} \Phi) \leq 0, \tag{28}$$

where $\dot{\boldsymbol{Q}}$ is zero when the system is at rest, and negative or negligible otherwise [34]. Therefore, the system is convex if $\partial_{\boldsymbol{X}} \partial_{\boldsymbol{X}} \Phi \geq 0$, which is valid when

$$\sum_j \frac{1}{R_j} + \sum_i \left(-\frac{P_{l,i}}{U_i^2} + \frac{1}{Z_{s,i}} + \frac{1}{Z_{z,i}} \right) \geq 0. \tag{29}$$

In the worst (allowed) case scenario there is only one droop source and constant power loads that all operate at the

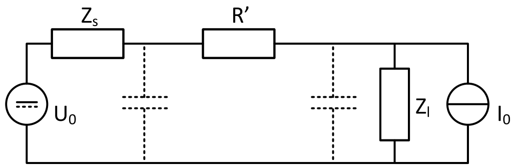

FIGURE 4. Incremental steady state circuit of a droop controlled source connected to a constant power load via an arbitrary dc distribution network.

minimum voltage $U_{\min}$. Therefore, convexity is ensured if

$$P_\Sigma \le \frac{U_{\min}^2}{Z_s + R_\Sigma}, \tag{30}$$

which is less strict than (17) as long as the minimum voltage is more than half the reference voltage.

The same result can be obtained using a more intuitive approach. Figure 4 shows in incremental (linearized) version of the example circuit, where the constant power load is replaced by a current source and a parallel impedance (see Section II-B).

This equivalent circuit converges to the equilibrium if a perturbation on the load voltage causes a larger change in source current than a change in the load current. In other words, if

$$\frac{1}{Z_s + R'} \ge \frac{1}{Z_l}, \tag{31}$$

$$Z_s + R' \le \frac{U_l^2}{P_l}, \tag{32}$$

$$P_l \le \frac{U_l^2}{Z_s + R'}, \tag{33}$$

which, in the worst case scenario, is equivalent to (30).

E. ASYMPTOTIC STABILITY

In addition to the convexity of the system it must be ensured that $\boldsymbol{Q} \succ 0$. From (24), it can be derived that this is the case when the diagonal entries of $\boldsymbol{Q}$ are positive definite [34]. It is clear that the choice of $\tau_{\max}$ ensures that $\tau_{\max}\boldsymbol{R} - \boldsymbol{L} \succ 0$. Furthermore, $\tau_{\max}\partial_{\boldsymbol{X}}\partial_{\boldsymbol{X}}G_0 + \boldsymbol{C}$ is positive definite if (for each node) it is true that

$$-\frac{\tau_{\max}P_{l,i}}{U_i^2} + \frac{\tau_{\max}}{Z_{s,i}} + \frac{\tau_{\max}}{Z_{z,i}} + C_i > 0, \tag{34}$$

which is always true for nodes to which no constant power nodes are connected. Furthermore, for nodes to which only constant power nodes are connected it is required that

$$C_i > \frac{\tau_{\max}P_{l,i}}{U_{min}^2}. \tag{35}$$

Intuitively this requirement can be explained by the time constants and damping of the system. If (35) is true, then the damping of each distribution line is more than the amplification of the constant power loads on oscillations in the system.

F. DC DISTRIBUTION SYSTEM STABILITY

In summary, if the minimum allowed voltage $U_{\min}$ is chosen to be more than half of the reference voltage U_0 there are two requirements or guidelines for the asymptotic stability of any dc distribution system.

Firstly, (17) ensures the existence and adequacy of the equilibrium, and that the system moves towards this equilibrium. Secondly, (34) ensures that there is sufficient damping on oscillations in the system. Furthermore, together these two requirements ensure asymptotic stability.

Although the two guidelines provide robust sufficient conditions for the global stability of the system an additional margin could be used to (further) reduce sensitivity to parameter deviations.

IV. DECENTRALIZED CONTROL STRATEGY FOR PLUG-AND-PLAY DC DISTRIBUTION GRIDS

This section presents a novel decentralized control strategy that ensures plug-and-play global stability and propriety of the voltage even when there is no communication infrastructure available.

From Section III it is clear that to ensure global stability and voltage propriety any dc distribution system must adhere to (17) and (34). It is straightforward to comply with (34) by requiring that the output capacitances of all constant power loads in the system are sized using (35). Here it is noteworthy that $\tau_{\max}$ is independent of the length and configuration of the distribution lines, and only depends on the type of cable (ratio of inductance and resistance).

However, it is less straightforward to comply with (17) since (for plug-and-play systems) the total load power, total resistance of the network, and the droop impedance is often variable or unknown. Therefore, instead of ensuring that the voltage remains above the minimum voltage via applying (17) directly, this is done by means of control.

A. CONVERTER BEHAVIOR

The converters in dc distribution grids can be categorized as source, load or hybrid converters. Although renewable energy sources are variable and uncertain by nature, due to maximum power point tracking algorithms, they exhibit constant power behavior in timeframes shorter than seconds [44]. Load converters exhibit behaviors such as constant impedance, constant power, constant current or a combination of these behaviors [45]. Hybrid converters supply or consume power depending on the system's voltage. Often hybrid converters exhibit constant power or impedance behavior.

B. DECENTRALIZED CONTROL STRATEGY

Previous research showed the advantages of dividing the acceptable voltage range into regions where the converters' mode of operation is varied [26]–[28], [32], [33]. However, unlike the decentralized control strategy presented in this paper, these methods do not ensure global stability, propriety of the voltage, and offer plug-and-play capabilities for dc distribution system (without utilizing communication).

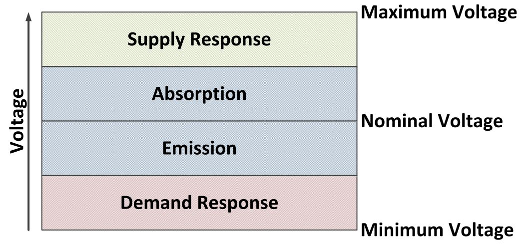

FIGURE 5. The different supply response, absorption, emission and demand response voltage regions for the decentralized control strategy.

To guarantee global stability and propriety of the voltage it must be ensured that the voltage never goes below the minimum voltage or above the maximum voltage. Therefore, the acceptable voltage range is divided into supply response, absorption, emission and demand response regions. An example of such a division of voltages is given in Figure 5. However, the different regions do not necessarily need to be divided proportionally.

The absorption and emission regions are the naturally desired regions of operation of the dc distribution grid. In these regions the load and source converters operate at constant power, while the hybrid converters (e.g., batteries) regulate the voltage. In the emission region, when the voltage is below the nominal voltage, the hybrid converters supply power to the grid. In this region, the hybrid converters ramp up their supplied current as the voltage reduces. In the absorption region, when the voltage is above the nominal voltage, the hybrid converters consume power from the grid. Analogously, the hybrid converters ramp up their consumed current as the voltage increases. When there are no hybrid converters in the network the system will always operate in the supply or demand response regions.

If the voltage enters the demand response region it means that the source and hybrid converters cannot cope with the power demand. Therefore, in the demand response region the load must be decreased. Loads either decrease their power gradually (e.g., by dimming lights) or switch off when a specified voltage is reached. The voltage at which the loads are switched off determines their priority. However, no load is allowed to consume power when the voltage is below the minimum voltage.

If the voltage reaches the supply response region the loads and hybrid converters cannot consume the power supplied by the sources. Therefore, in this region the power supply must be reduced. Similar to the demand response, the sources either gradually decrease their output power or switch off at a specified voltage. However, no source is allowed to supply power when the voltage is above the maximum voltage.

An example of the behavior in the voltage regions for source, load and hybrid converters is shown in Figure 6. In this example the source and load converters' power is ramped down in the supply and demand response regions.

C. CONVERTER GUIDELINES

The decentralized control strategy from the previous subsection ensures plug-and-play global stability and voltage propriety. However, some additional guidelines for the converter behavior are desirable if some additional knowledge about the system is available.

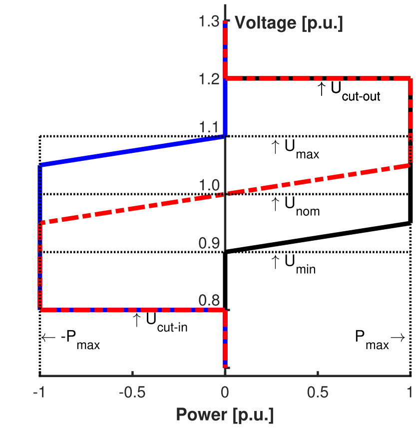

FIGURE 6. Example of a source (blue), load (black) and hybrid (red) converters' voltage-current characteristic that complies with the decentralized control strategy.

Firstly, natural voltage and current transients occur during changes in the system. To prevent these transients from negatively affecting control decisions, changes should be ramped over a significantly longer time period than the slowest time constant (of distribution lines and capacitors) in the system. Consequently, transients in the system will be significantly damped before a final control decision is made.

Secondly, while a change is ramped, a voltage drop is incurred on over the system's inductances. This voltage drop is equal to the system's equivalent inductance times the current rate of change. The voltage drop dictates the error between the measured state and the steady state, but also affects the maximum overshoot of the steady state. Therefore, the ramp rate should be chosen to achieve a desired accuracy.

Thirdly, to prevent repeated transitions between control states (such as the connection or disconnection of a load), some form of hysteresis is recommended. For example, the voltages for disconnecting and connecting a load should be (slightly) offset.

To illustrate the reason for the first two converter behavior guidelines a simple system shown in Figure 7 is used. However, this approach can be used to analyze more complex systems yielding similar results.

The source's voltage U is assumed to be constant, while the load's current I is variable. Since the load's control decisions

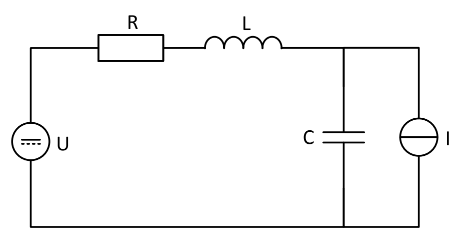

FIGURE 7. Simple system used to illustrate the necessity of the guidelines on the converter behavior.

are made on the local voltage, the voltage of the capacitor U_c is of interest. The transfer function of the capacitor voltage as function of the load current I is

$$U_c = \frac{-1}{sC + \frac{1}{sL+R}} I. \tag{36}$$

The poles of this transfer function are given by

$$p_{1,2} = \frac{-R}{2L} \pm \sqrt{\frac{R^2}{4L^2} - \frac{1}{CL}}. \tag{37}$$

Moreover, these poles are bounded by two different sets of poles. Firstly, when the capacitance is negligible the poles are approximated by

$$p_{1,2} \approx \frac{-R}{L}. \tag{38}$$

Secondly, when the inductance is negligible the poles are approximated by

$$p_{1,2} \approx \frac{-1}{RC}. \tag{39}$$

Consequently, the transients in the system are bounded by the time constant of the distribution line (L/R) and capacitance (RC). To prevent transients significantly affecting control decisions, it is recommended that, for more complex systems, any change is ramped over a significantly longer period than the slowest time constant of the system.

When the current source I is ramped with a ramp rate a the dynamic response of the capacitor's voltage can be found by using the inverse Laplace transform

$$U_c(t) = \mathcal{L}^{-1}\left(\frac{a}{s^2} \cdot \frac{-1}{sC + \frac{1}{sL+R}}\right), \tag{40}$$

$$U_c(t) = U_c(0) + a(-Rt - L + CR^2 + e^{-\frac{Rt}{2L}} f(t)), \tag{41}$$

$$f(t) = \frac{\sqrt{C}R\,(3L - CR^2)\sinh\left(\frac{t\sqrt{CR^2-4L}}{2\sqrt{C}L}\right)}{\sqrt{CR^2-4L}} + \left(L - CR^2\right)\cosh\left(\frac{t\sqrt{CR^2-4L}}{2\sqrt{C}L}\right). \tag{42}$$

In (41), $e^{-\frac{Rt}{2L}} f(t)$ represents the transients in the system which are damped out over time. Furthermore, $U_c(0) - aRt$ represents the steady steady state of the system for the load current $I(0) + at$. Moreover, $-aL + aCR^2$ represents the offset between the steady state of the system and the perceived voltage during the ramping of the current.

In the worst case, the offset of scenario the capacitor's voltage from the steady state can therefore be approximated by aL. Therefore, a desired accuracy of the converter's controller can be achieved by choosing an appropriate ramp rate a. For more complex systems the accuracy can be ensured by assessing the equivalent inductance (in the worst case the total inductance) of the system.

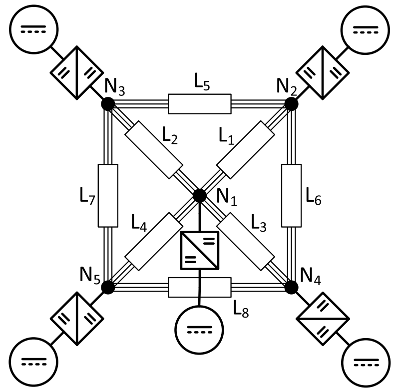

FIGURE 8. Example system for the simulation of the stability and the presented decentralized control strategy.

TABLE 1. Distribution line parameters for the example analyses.

R_L $[\Omega]$	L_L $[mH]$	C_L $[\mu F]$	G_L $[mS]$
1	0.25	0.5	0

V. SIMULATION EXAMPLES OF THE STABILITY AND DECENTRALIZED CONTROL STRATEGY

In this section several simulations are performed to illustrate the stability and the behavior of the presented decentralized control strategy under various scenarios. For all the simulations the simple bipolar dc microgrid shown in Figure 8 is used. However, the principles are scalable and work for larger dc distribution systems.

For the simulations it is assumed that the different distribution lines are identical, and have the parameters given in Table 1, which are parameters of typical distribution lines with a length of 1 km. Furthermore, it is assumed that the output capacitance of every converter is 50 μF. Additionally, the nominal voltage of the grid is $\pm$350 V with a margin of $\pm 10\%$. Consequently, the minimum and maximum allowed voltages of the grid are $\pm$315 V and $\pm$385 V respectively.

Since the converter capacitance, minimum voltage and time constants of the distribution lines are know, the maximum power of a load converter in this system can be calculated from (35) to be 20 kW. Accordingly, the system will be stable if the load converters switch off at the minimum voltage and do not consume more than 20 kW.

A. GRID CONNECTED DC MICROGRID: IDEAL CASE

The first example simulation is a dc distribution grid where all the common elements are present. Firstly, at node N_1 the grid is connected to a larger stiff grid. This grid connected converter is droop controlled with a reference voltage of 700 V ($\pm$350 V) and a droop impedance of 4 Ω. Secondly, constant power loads are connected at nodes N_2, N_3, and N_4. The reference powers of these constant power loads over time are shown in Table 2. Lastly, at N_5 a converter of photovoltaic panels with maximum power point tracking is connected. The

TABLE 2. Reference power of the constant power loads and the PV source.

t [ms]	P_2^* [W]	P_3^* [W]	P_4^* [W]	P_5^* [W]
0	0	0	0	-3900
5	1500	0	0	-3900
10	1500	3000	0	-3900
15	1500	3000	2000	-3900
20	1500	3000	2000	-2500

output power over time of this PV converter is also shown in Table 2.

To add complexity, the loads and source are assumed to not ramp their output power in the response regions but switch off at specified voltages. In this scenario the loads at N_2, N_3 and N_4 are switched off at 315 V, 325 V and 320 V respectively. Consequently the load at N_2 has the highest priority and the load at N_3 has the lowest priority. Furthermore, the PV source is switched off at 385 V.

The simulation results of this ideal scenario, when all the elements are active, are given in Figure 9. From the simulation results it is clear that the system is indeed stable and that the voltage remains in the absorption and emission regions. At 10 ms the voltage moves from the absorption into the emission region since the total power of the loads exceeds the supplied power of the PV source. In this scenario the hybrid converter at N_1 ensures that all the excess or deficit in power is balanced by the regional grid.

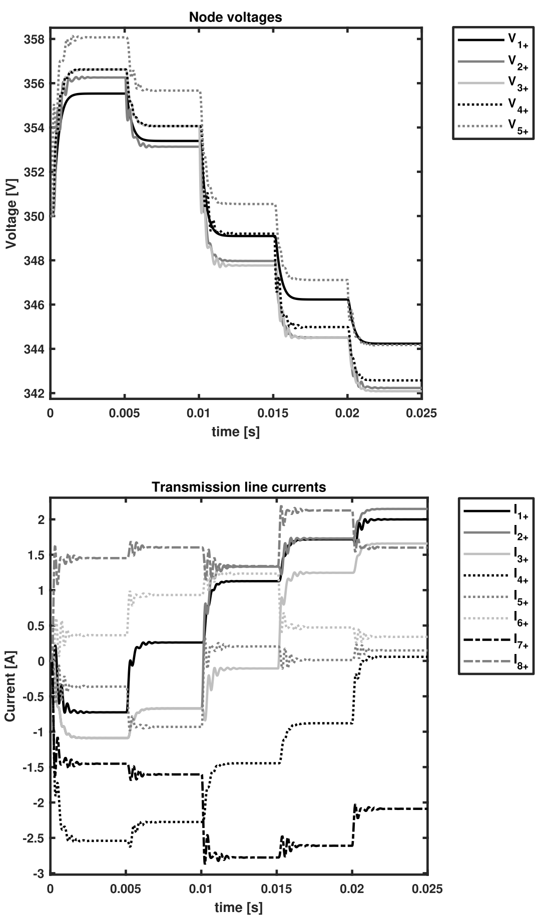

FIGURE 9. Simulation results for the grid connected dc microgrid in the ideal case when all elements are active.

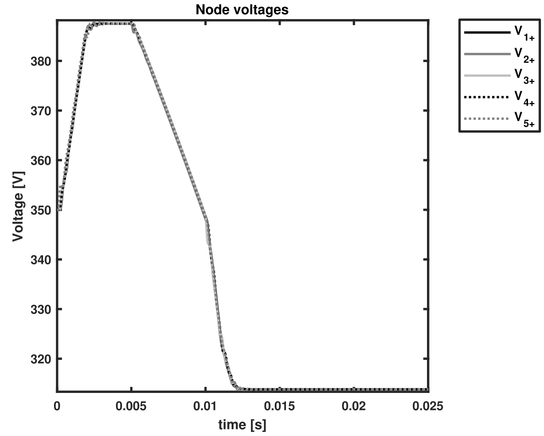

FIGURE 10. Simulation results for the isolated dc microgrid in the worst case when there is no available flexibility in the grid.

B. ISOLATED DC MICROGRID: WORST CASE

In the previous simulation example it was assumed that the microgrid was connected to a stiff grid via a power electronic converter. However, in this scenario this converter is non-operational. This situation can, for example, occur during an outage of a regional grid. Other than the grid connected converter, this scenario is identical to the previous scenario.

The simulation results of this scenario are given in Figure 10. This scenario is the worst case scenario since all the loads and the source either operate at their reference power or no power. Therefore, the microgrid does not have any form of flexibility and no match in supply and demand can be found (no combination of loads exactly equals the source power).

Although the system is stable, the system is either at the maximum or minimum voltage. This decentralized control strategy can only find a solution if there exists a match in supply and demand. If there is no flexibility in any source, load or hybrid node in the system it is unlikely that such a solution will be found.

C. ISOLATED DC MICROGRID: SOURCE-SIDE FLEXIBILITY

In the previous scenario there were no nodes that provided flexibility to the grid and therefore the control strategy could not find a match between supply and demand. This scenario is identical to the previous scenario, however in this simulation source-side flexibility is introduced by ramping the source's power in the supply response region (as shown in Figure 6). The results of this simulation are shown in Figure 11.

Since there is flexibility, the control strategy is able to find a suitable match of supply and demand. Between 0 and 5 ms, when there is no load connected, the source power is ramped down completely. Afterwards, when the first load is switched on a steady state is reached at 10 ms. Furthermore, when the

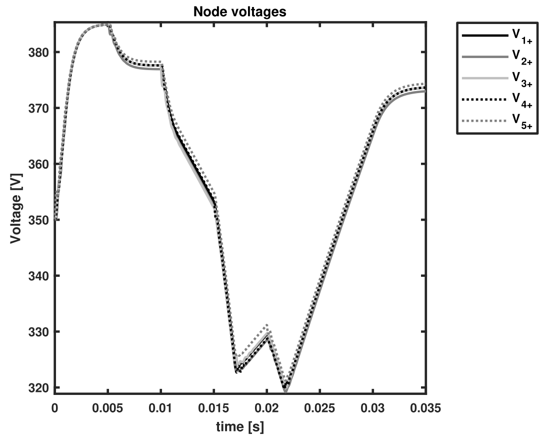

FIGURE 11. Simulation results for the isolated dc microgrid in the scenario where the source is providing flexibility to the grid.

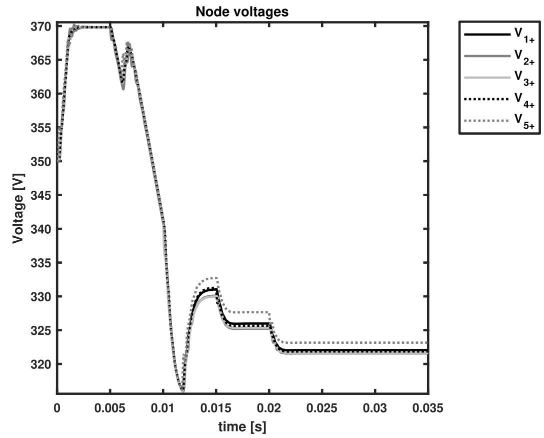

FIGURE 12. Simulation results for the isolated dc microgrid in the scenario where the loads are providing flexibility to the grid.

load power exceeds the source's power, the drop in voltage results in loads being switched off completely until a match is found between supply and demand. Twice a load is switched off, once when an additional load is switched on (at 15 ms) and once when the source power is reduced (at 20 ms).

D. ISOLATED DC MICROGRID: LOAD-SIDE FLEXIBILITY

The last scenario is, again, almost identical to the second scenario, however in this simulation load-side flexibility is introduced (instead of source-side flexibility) by ramping down loads in the demand response voltage region (as shown in Figure 6). Furthermore, the source's control is set to re-attempt connection to the dc grid every 5 ms. The results of this simulation are shown in Figure 12.

Also in this case, the system is stable and the decentralized control strategy finds a suitable match of supply and demand. Between 0 and 10 ms the load power is not sufficient to consume the non-flexible source power. Therefore, the source is switched off and no power is consumed by the loads. However, at 10 ms a match between supply and demand is found since the total demand exceeds the total supply. Furthermore, in subsequent changes the control strategy finds a suitable solution.

VI. DISCUSSION

The stability guidelines and decentralized control strategy presented in this paper ensure global stability, that the voltage stays between the desired bounds and maximization of the energy utilization. Compared to previous publications, the presented stability guidelines and decentralized control strategy do not require communication and only require minimal knowledge of the system to achieve these goals.

For example, droop based strategies require communication or a known topology and system parameters [17]–[22]. Strategies that adapt the virtual impedance (or operating mode) reduce this dependency but do not eliminate it [23]–[29]. Furthermore, plug-and-play strategies exist but still require some form of communication or that the different (possible) system topologies and/or parameters are known [26], [31]–[33]. On the other hand, the presented method only requires an estimate of the worst time constant of the lines in the system ($\tau_{\max}$). Moreover, this time constant is only dependent on the type of cable and not of the length or configuration. Therefore, the sensitivity of the presented method to line impedance is low.

In the previous section a few examples a few examples of different scenarios utilizing the control strategy for plug-and-play dc distribution systems without communication were analyzed of different scenarios utilizing the control strategy for plug-and-play dc distribution systems without communication. In general, the control strategy will find a suitable solution and stable when flexibility is available in the system. The flexibility can be provided by hybrid converters (e.g., grid tied or battery converters), source converters or load converters.

Flexibility provided by load converters can be achieved by reducing the load (e.g., dimmable lighting) or by (temporarily) supplying the load by local storage. Furthermore, flexibility in source converters can be achieved, for example, by going outside of the maximum power point for photovoltaic and wind energy sources. Alternatively, the excess power can be (temporarily) dumped into a resistive circuit.

An optimal situation is when there is more than one type of flexibility present in the grid. In this case the available flexibility from hybrid converters will be utilized first to compensate the excess or deficit in power. If this flexibility is not sufficient, the flexibility in the respective demand or supply response regions will start playing a role.

When non-flexible loads and sources are used they switch off at a specified voltage, where the relative voltage to other loads/sources determines its priority. However, resistive voltage drops over the distribution lines may cause an offset in measured voltages of the converters (and may cause a shift in priority). Nevertheless, in general, these voltage drops are negligible in distribution systems when the switch-off voltages are chosen with a reasonable disparity.

VII. CONCLUSION

A significant challenge for dc distribution grids is the global stability and decentralized control of plug-and-play grids. Previous research relied mostly on the system being well defined or some form of communication. The contributions of this paper are easy-to-use global stability guidelines, a decentralized control strategy that implements these stability guidelines, and supplementary converter guidelines for plug-and-play dc distribution grids that are (temporarily) without communication. Moreover, minimal knowledge of the system is required.

A model of dc distribution systems was presented and, by using this model and a Brayton-Moser representation of the system, stability guidelines were derived by finding a suitable Lyapunov candidate function. These stability guidelines resulted in two easy-to-use requirements on plug-and-play dc distribution systems. Firstly, the output capacitance of constant power loads must be sized according to its power, the minimum allowed voltage and the system's slowest time constant. This slowest time constant is the only required information of the system and exclusively depends on the type of cable and not on the length or configuration of the distribution lines. Secondly, constant power loads must be disconnected from the grid when the local voltage goes below the minimum allowed voltage.

The stability guidelines were implemented in a decentralized control strategy. Four regions of operation were defined within the allowable voltage range: the supply response, absorption, emission and demand response regions. In general converters are expected to switch off or ramp down their output power at designated voltages. Furthermore, additional guidelines were established for the converters if additional knowledge about the system is available to improve the transient behavior of the system. These converter guidelines establish the maximum current rate of change and minimum ramp time of changes in the system to achieve a required accuracy of the system.

Several example simulations were performed to demonstrate the stability of the system and the behavior of the control strategy and guidelines in different scenarios. The decentralized control strategy aims to find a match between supply and demand in the system. However, to achieve such a match the control strategy requires some form of flexibility. If no flexibility is present in the system no power will be exchanged between sources and loads (unless supply, demand and losses are perfectly matched). Various scenarios where the flexibility is provided by the source, load and a stiff grid connection were investigated. These scenarios illustrated that any form of flexibility is sufficient for the system to operate.

The work presented in this paper can form a basis for the stability of plug-and-play dc distribution systems and their standards. In future work, the decentralized control strategy could be expanded upon by implementing an algorithm that arranges the disconnection and connection of loads with identical priority, and by further improving stability and reliability when communication is available.

REFERENCES

[1] A. Ipakchi and F. Albuyeh, "Grid of the future," *IEEE Power Energy Mag.*, vol. 7, no. 2, pp. 52–62, Mar. 2009.

[2] L. Meng *et al.*, "Review on control of DC microgrids and multiple microgrid clusters," *IEEE J. Emerg. Sel. Topics Power Electron.*, vol. 5, no. 3, pp. 928–948, Sep. 2017.

[3] A. Bidram and A. Davoudi, "Hierarchical structure of microgrids control system," *IEEE Trans. Smart Grid*, vol. 3, no. 4, pp. 1963–1976, Dec. 2012.

[4] J.-C. Kim, S.-M. Cho, and H.-S. Shin, "Advanced power distribution system configuration for smart grid," *IEEE Trans. Smart Grid*, vol. 4, no. 1, pp. 353–358, Mar. 2013.

[5] L. Mackay, T. Hailu, L. Ramírez-Elizondo, and P. Bauer, "Towards a DC distribution system—Opportunities and challenges," in *Proc. IEEE 1st Int. Conf. DC Microgrids (ICDCM)*, Jun. 2015, pp. 215–220.

[6] J. Driesen and K. Visscher, "Virtual synchronous generators," in *Proc. IEEE Power Energy Soc. Gen. Meeting Convers. Delivery Elect. Energy 21st Century*, Jul. 2008, pp. 1–3.

[7] J. Morren, S. W. H. de Haan, and J. A. Ferreira, "Contribution of DG units to primary frequency control," in *Proc. Int. Conf. Future Power Syst.*, Nov. 2005, p. 6.

[8] N. Hatziargyriou, H. Asano, R. Iravani, and C. Marnay, "Microgrids," *IEEE Power Energy Mag.*, vol. 5, no. 4, pp. 78–94, Jul. 2007.

[9] F. M. F. Flaih, X. Lin, M. K. Abd, S. M. Dawoud, Z. Li, and O. S. Adio, "A new method for distribution network reconfiguration analysis under different load demands," *Energies*, vol. 10, no. 4, p. 455, 2017.

[10] A. Q. Huang, M. L. Crow, G. T. Heydt, J. P. Zheng, and S. J. Dale, "The future renewable electric energy delivery and management (FREEDM) system: The energy Internet," *Proc. IEEE*, vol. 99, no. 1, pp. 133–148, Jan. 2011.

[11] J. Kumagai, "The rise of the personal power plant," *IEEE Spectr.*, vol. 51, no. 6, pp. 54–59, Jun. 2014.

[12] J. M. Guerrero, J. C. Vasquez, J. Matas, L. G. de Vicuna, and M. Castilla, "Hierarchical control of droop-controlled AC and DC microgrids—A general approach toward standardization," *IEEE Trans. Ind. Electron.*, vol. 58, no. 1, pp. 158–172, Jan. 2011.

[13] V. Arcidiacono, A. Monti, and G. Sulligoi, "Generation control system for improving design and stability of medium-voltage DC power systems on ships," *IET Elect. Syst. Transp.*, vol. 2, no. 3, pp. 158–167, Sep. 2012.

[14] D. M. Larruskain, I. Zamora, O. Abarrategui, and Z. Aginako, "Conversion of AC distribution lines into DC lines to upgrade transmission capacity," *Electr. Power Syst. Res.*, vol. 81, no. 7, pp. 1341–1348, 2011.

[15] L. Mackay, T. G. Hailu, G. C. Mouli, L. Ramírez-Elizondo, J. A. Ferreira, and P. Bauer, "From DC nano- and microgrids towards the universal DC distribution system—A plea to think further into the future," in *Proc. IEEE Power Energy Soc. Gen. Meeting*, Jul. 2015, pp. 1–5.

[16] T. Hakala, T. Lähdeaho, and P. Järventausta, "Low-voltage DC Distribution—Utilization potential in a large distribution network company," *IEEE Trans. Power Del.*, vol. 30, no. 4, pp. 1694–1701, Aug. 2015.

[17] B. T. Irving and M. M. Jovanovic, "Analysis, design, and performance evaluation of droop current-sharing method," in *Proc. 15th Annu. IEEE Appl. Power Electron. Conf. Expo. (APEC)*, vol. 1, Feb. 2000, pp. 235–241.

[18] P. Karlsson and J. Svensson, "DC bus voltage control for a distributed power system," *IEEE Trans. Power Electron.*, vol. 18, no. 6, pp. 1405–1412, Nov. 2003.

[19] M. Lee, D. Chen, K. Huang, C. W. Liu, and B. Tai, "Modeling and design for a novel adaptive voltage positioning (AVP) scheme for multiphase VRMs," *IEEE Trans. Power Electron.*, vol. 23, no. 4, pp. 1733–1742, Jul. 2008.

[20] A. Maknouninejad, Z. Qu, F. L. Lewis, and A. Davoudi, "Optimal, nonlinear, and distributed designs of droop controls for DC microgrids," *IEEE Trans. Smart Grid*, vol. 5, no. 5, pp. 2508–2516, Sep. 2014.

[21] F. Chen, R. Burgos, D. Boroyevich, and W. Zhang, "A nonlinear droop method to improve voltage regulation and load sharing in DC systems," in *Proc. IEEE 1st Int. Conf. DC Microgrids (ICDCM)*, Jun. 2015, pp. 45–50.

[22] P. Prabhakaran, Y. Goyal, and V. Agarwal, "Novel nonlinear droop control techniques to overcome the load sharing and voltage regulation issues in DC microgrid," *IEEE Trans. Power Electron.*, vol. 33, no. 5, pp. 4477–4487, May 2017.

[23] Z. Ye, D. Boroyevich, K. Xing, and F. C. Lee, "Design of parallel sources in DC distributed power systems by using gain-scheduling technique," in *Proc. 30th Annu. IEEE Power Electron. Specialists Conf.*, Aug. 1999, pp. 161–165.

[24] H. Kakigano, A. Nishino, and T. Ise, "Distribution voltage control for DC microgrid with fuzzy control and gain-scheduling control," in *Proc. 8th Int. Conf. Power Electron. ECCE Asia*, May 2011, pp. 256–263.

[25] T. V. Vu, D. Perkins, F. Diaz, D. Gonsoulin, C. S. Edrington, and T. El-Mezyani, "Robust adaptive droop control for DC microgrids," *Electr. Power Syst. Res.*, vol. 146, pp. 95–106, Jan. 2017.

[26] Y. Gu, X. Xiang, W. Li, and X. He, "Mode-adaptive decentralized control for renewable DC microgrid with enhanced reliability and flexibility," *IEEE Trans. Power Electron.*, vol. 29, no. 9, pp. 5072–5080, Sep. 2014.

[27] A. Khorsandi, M. Ashourloo, and H. Mokhtari, "A decentralized control method for a low-voltage DC microgrid," *IEEE Trans. Energy Convers.*, vol. 29, no. 4, pp. 793–801, Dec. 2014.

[28] H. Li, C. Liu, G. Li, and R. Iravani, "An enhanced DC voltage droop-control for the VSC–HVDC Grid," *IEEE Trans. Power Syst.*, vol. 32, no. 2, pp. 1520–1527, Mar. 2017.

[29] C. Dierckxsens, K. Srivastava, M. Reza, S. Cole, J. Beerten, and R. Belmans, "A distributed DC voltage control method for VSC MTDC systems," *Electr. Power Syst. Res.*, vol. 82, no. 1, pp. 54–58, 2012.

[30] M. Tucci, S. Riverso, J. C. Vasquez, J. M. Guerrero, and G. Ferrari-Trecate, "A decentralized scalable approach to voltage control of DC islanded microgrids," *IEEE Trans. Control Syst. Technol.*, vol. 24, no. 6, pp. 1965–1979, Nov. 2016.

[31] A. H. Etemadi, E. J. Davison, and R. Iravani, "A decentralized robust control strategy for multi-DER microgrids—Part I: Fundamental concepts," *IEEE Trans. Power Del.*, vol. 27, no. 4, pp. 1843–1853, Oct. 2012.

[32] D. Chen, L. Xu, and L. Yao, "DC voltage variation based autonomous control of DC microgrids," *IEEE Trans. Power Del.*, vol. 28, no. 2, pp. 637–648, Apr. 2013.

[33] Y. Gu, W. Li, and X. He, "Frequency-coordinating virtual impedance for autonomous power management of DC microgrid," *IEEE Trans. Power Electron.*, vol. 30, no. 4, pp. 2328–2337, Apr. 2015.

[34] J. A. Belk, W. Inam, D. J. Perreault, and K. Turitsyn, "Stability and control of ad hoc DC microgrids," in *Proc. IEEE 55th Conf. Decis. Control (CDC)*, Dec. 2016, pp. 3271–3278.

[35] N. H. van der Blij, L. M. Ramírez-Elizondo, P. Bauer, and M. T. J. Spaan, "Design guidelines for stable DC distribution systems," in *Proc. IEEE 2nd Int. Conf. DC Microgrids (ICDCM)*, Jun. 2017, pp. 279–284.

[36] N. H. van der Blij, L. M. Ramírez-Elizondo, M. T. J. Spaan, and P. Bauer, "A state-space approach to modelling DC distribution systems," *IEEE Trans. Power Syst.*, vol. 33, no. 1, pp. 943–950, Jan. 2018.

[37] C. R. Paul, *Analysis of Multiconductor Transmission Lines*, 2nd ed. Hoboken, NJ, USA: Wiley, 2007.

[38] A. Emadi, A. Khaligh, C. H. Rivetta, and G. A. Williamson, "Constant power loads and negative impedance instability in automotive systems: Definition, modeling, stability, and control of power electronic converters and motor drives," *IEEE Trans. Veh. Technol.*, vol. 55, no. 4, pp. 1112–1125, Jul. 2006.

[39] A. Kwasinski and C. N. Onwuchekwa, "Dynamic behavior and stabilization of DC microgrids with instantaneous constant-power loads," *IEEE Trans. Power Electron.*, vol. 26, no. 3, pp. 822–834, Mar. 2011.

[40] N. H. van der Blij, L. M. Ramírez-Elizondo, M. T. J. Spaan, and P. Bauer, "Stability of DC distribution systems: An algebraic derivation," *Energies*, vol. 10, no. 9, p. 1412, 2017.

[41] S. Bolognani and S. Zampieri, "On the existence and linear approximation of the power flow solution in power distribution networks," *IEEE Trans. Power Syst.*, vol. 31, no. 1, pp. 163–172, Jan. 2016.

[42] R. Brayton and J. Moser, "Some results on the stability of nonlinear networks containing negative resistances," *IEEE Trans. Circuit Theory*, vol. 11, no. 1, pp. 165–167, Mar. 1964.

[43] D. Jeltsema and J. M. A. Scherpen, "Multidomain modeling of nonlinear networks and systems," *IEEE Control Syst.*, vol. 29, no. 4, pp. 28–59, Aug. 2009.

[44] R. A. Mastromauro, M. Liserre, and A. D'Aquila, "Control issues in single-stage photovoltaic systems: MPPT, current and voltage control," *IEEE Trans. Ind. Informat.*, vol. 8, no. 2, pp. 241–254, May 2012.

[45] D. Salomonsson and A. Sannino, "Load modelling for steady-state and transient analysis of low-voltage DC systems," *IET Electr. Power Appl.*, vol. 1, no. 5, pp. 690–696, Sep. 2007.

NILS H. VAN DER BLIJ (S'16) was born in Leiden, The Netherlands, in 1990. He received the bachelor's and master's degrees in electrical engineering from Delft University of Technology in 2011 and 2013, respectively. He is currently pursuing the Ph.D. degree with a focus on the management and control of dc distribution grids. His research experience includes Scarabee, Philips, Cambridge University, and the Delft University of Technology. His specializations lie in the field of dc distribution grids, electrical machines and drives, and sustainable energy generation.

LAURA M. RAMIREZ-ELIZONDO (M'06) received the bachelor's degree in electrical engineering and the bachelor's degree in music with a major in piano from the Universidad de Costa Rica in 2003 and the M.Sc. degree (Hons.) in electrical power engineering and the Ph.D. degree in electrical engineering from the Delft University of Technology in 2007 and 2013, respectively. She is currently an Assistant Professor with the DC Systems, Energy Conversion and Storage Group, Delft University of Technology.

MATTHIJS T. J. SPAAN (S'05–M'12) received the M.Sc. degree in artificial intelligence and the Ph.D. degree in computer science from the University of Amsterdam in 2002 and 2006, respectively. He is currently an Associate Professor of computer science at Delft University of Technology, The Netherlands.

PAVOL BAUER (SM'07) is currently a Full Professor with the Department of Electrical Sustainable Energy, Delft University of Technology, and the Head of the DC Systems, Energy Conversion and Storage Group. He has published over 72 journal and about 300 conference papers in his field (with a H factor Google Scholar 30 and Web of Science 18). He has authored or co-authored of eight books, holds four international patents, and organized several tutorials at the international conferences. He has worked on many projects for industry concerning wind and wave energy and power electronic applications for power systems such as Smarttrafo and HVDC and LV DC systems and projects for smart cities, such as PV charging of electric vehicles, PV and storage integration, contactless charging, and he participated in several Leonardo da Vinci and H2020 EU projects as a Project Partner (ELINA, INETELE, E-Pragmatic) and a Coordinator (PEMCWebLab.com-Edipe, SustEner, Eranet DCMicro). He is the Former Chairman of the Benelux IEEE Joint Industry Applications Society, the Power Electronics and Power Engineering Society Chapter, the Chairman of the Power Electronics and Motion Control (PEMC) Council, a member of the Executive Committee of European Power Electronics Association, and also a member of the International Steering Committee at numerous conferences.